Atomic mass relations of mirror nuclei

S. T. Guo, Y. X. Yu, Z. Wang, G. J. Fu,* and Z. Z. Ren
School of Physics Science and Engineering, Tongji University, Shanghai 200092, China

(Received 10 October 2023; accepted 1 December 2023; published 2 January 2024)

In this paper we study the mass relation of mirror nuclei with our focus on pairing and shell effects in the Coulomb energy. We present an accurate mass formula for neutron-deficient nuclei with mass number $A > 20$ that achieves a root-mean square deviation (RMSD) of 70 keV when compared to experimental data from AME2020, and the RMSD further diminishes to 49 keV when excluding five nuclei with experimental uncertainties larger than 100 keV. Based on the mass formula, we predict 174 atomic masses near the proton drip line with $20 < A < 115$, and tabulate the results in the Supplemental Material of this paper.

DOI: 10.1103/PhysRevC.109.014304

I. INTRODUCTION

Nuclear mass (or alternatively nuclear binding energy) plays an important role in nuclear physics and astrophysics [1,2]. Nuclear mass measurements not only challenge nuclear models but also yield crucial insights into nucleon-nucleon interactions, shell evolution, shape-phase transition, pairing, and clustering. Accurate mass measurements and theoretical predictions provide us with valuable information on elemental abundance, nucleosynthesis pathways, properties of compact stars, and astrophysical energy production.

Numerous efforts have been devoted to improving the theoretical predictions of nuclear mass. Various global mass models and formulas have been significantly improved, including the famous Duflo-Zuker model [3,4], the Skyrme-Hartree-Fock-Bogoliubov theory [5,6], the improved Weizsäcker-Skyrme mass formula [7,8], the finite-range droplet model, and finite-range liquid drop model [9]. Local mass relations have also been found to exhibit a small root-mean square deviation (RMSD), such as the Garvey-Kelson mass relation [10–13], the Audi-Wasptra (AW) extrapolation method [14], and the mass relation of the residual proton-neutron interaction [15–18]. It is worth noting that while these global and local approaches achieve a high level of accuracy (typically with RMSDs of 100–500 keV) for a wide range of nuclei, they tend to be less accurate for light nuclei. Most theoretical predictions exhibit deviations larger than 400 keV compared to experimental data for nuclei with $N < Z < 40$. A comprehensive review is presented in Ref. [19].

From another perspective, mass relations between mirror nuclei have been studied by calculating the Coulomb energy based on the assumption that low-lying states of atomic nuclei approximately conserve isospin symmetry. For example, Ormand [20] studied the Coulomb displacement energy (CDE) using the isobaric multiplet mass equation [21]. Brown *et al.* made use of the Skyrme-Hartree-Fock calculation, incorporating charge-symmetry breaking forces, to report the CDE results with an RMSD of ≈100 keV in the mass region $A = 41$–59 [22,23]. Bao *et al.* described the mass difference between mirror nuclei using an empirical Coulomb energy formula, achieving RMSDs of 120–290 keV [24]. Zong *et al.* proposed several formulas of local mass relations for mirror nuclei based on the residual proton-neutron interactions and one-nucleon separation energy with RMSDs of 70–140 keV [25–27]. Ma *et al.* emphasized the presence of local correlations in these formulas, which have been found to improve the accuracy of mass predictions [28].

In this paper, we revisit the mass relation of mirror nuclei discussed in Ref. [24] by considering pairing and shell effects in the Coulomb energy. We propose a simple mass formula for neutron-deficient nuclei, which achieves an RMSD of 70 keV for nuclei with mass numbers $A > 20$. We demonstrate the predictive capability of our formula. This paper is organized as follows. In Sec. II, we discuss pairing and shell effects in the atomic mass difference between mirror nuclei, and present our formula. In Sec. III, we make use of the formula to predict masses of neutron-deficient nuclei. Finally, in Sec. IV, we summarize our results.

II. ATOMIC MASS DIFFERENCE OF MIRROR NUCLEI

In this paper we use $M_{\rm N}(N,Z)$, $M_{\rm A}(N,Z)$, and $B(N,Z)$ to denote the nuclear mass, atomic mass, and nuclear binding energy of a nucleus with N neutrons and Z protons, respectively. The nuclear masses $M_{\rm N}(N,Z)$ can be calculated from the atomic ones $M_{\rm A}(N,Z)$ as follows:

$$M_{\rm N}(N,Z) = M_{\rm A}(N,Z) - Z \times M_e + B_e(Z), \tag{1}$$

where M_e is the electron mass, and $B_e(Z)$ is the electron binding energy evaluated by [1]

$$B_e(Z) = 14.4381 Z^{2.39} + 1.55468 \times 10^{-6} Z^{5.35} \text{ eV}. \tag{2}$$

*Corresponding author: gjfu@tongji.edu.cn

The nuclear binding energy $B(N, Z)$ is evaluated by the Weizsäcker formula, i.e.,

$$B(N, Z) = a_v A - a_s A^{2/3} - a_c Z(Z-1)A^{-1/3} - a_{sym}(N-Z)^2 A^{-1} + a_{pair}\delta_{N,Z}, \quad (3)$$

where $A = N + Z$ is the mass number of the nucleus, and a_v, a_s, a_c, a_{sym}, and a_{pair} are the coefficients of the volume energy term, surface energy term, Coulomb energy term, symmetry energy term, and pairing energy term, respectively.

Using Eqs. (1) and (3), one obtains a simple formula of atomic mass difference between two corresponding mirror nuclei with neutron and proton numbers $(N, Z) = (K - k, K)$ and $(K, K - k)$ as follows:

$$\Delta_k(K) \equiv M_A(K-k, K) - M_A(K, K-k) = a_c k(A-1)A^{-1/3} + f_k(K). \quad (4)$$

Here, K represents the larger of the neutron and proton numbers of the nuclei, and k represents the difference between the neutron and proton numbers. The mass number, A, can then be expressed as $A = 2K - k$. The term $f_k(K)$ is a parameter-free function that relies solely on K and k:

$$f_k(K) \equiv k(M_p + M_e - M_n) + B_e(K-k) - B_e(K), \quad (5)$$

where M_p and M_n are proton and neutron masses. From Eq. (4), one sees the Coulomb energy term in the Weizsäcker formula significantly influences the mass difference of mirror nuclei.

Unfortunately, the RMSD of the mass difference, as calculated using Eq. (4), is not small (typically ≈310 keV) compared to the experimental data from AME2020 [29]. This discrepancy is attributed to the oversimplification of Eq. (3) in representing the Coulomb energy contribution to the nuclear binding energy. To address this issue, we incorporate a more sophisticated Coulomb energy formula

$$B_c(N, Z) = -a_c Z(Z-1)A^{-1/3} - a_{ex}Z^{4/3}A^{-1/3} - a_p(-1)^Z A^{-1}. \quad (6)$$

The first term in the above formula, which is the same as the Coulomb energy term in Eq. (3), is commonly referred to as the direct term. The second term is known as the exchange term, which arises from the antisymmetrization of the proton wave function in quantum many-body models, such as the Fermi gas model. The coefficient a_{ex} derived from the Fermi gas model is precisely equal to $-\frac{5}{4}(\frac{3}{2\pi})^{2/3}a_c$. It should be noted that the relation between coefficients a_{ex} and a_c is model dependent. Therefore, in this work, we consider a_{ex} as a free parameter. The third term is called the Coulomb pairing term, which originates from the nuclear pairing effect. This effect is characterized by the nuclear pairing force, which causes nucleons around the Fermi sea to form spin $J = 0$ pairs at shorter distances, resulting in an increased Coulomb repulsion between them.

Assuming the Coulomb energy formula of Eq. (6), we have

$$\Delta_k(K) \approx a_c k(A-1)A^{-1/3} + f_k(K) + \frac{2^{5/3}}{3}a_{ex}k + a_p(1-(-1)^k)(-1)^K A^{-1}. \quad (7)$$

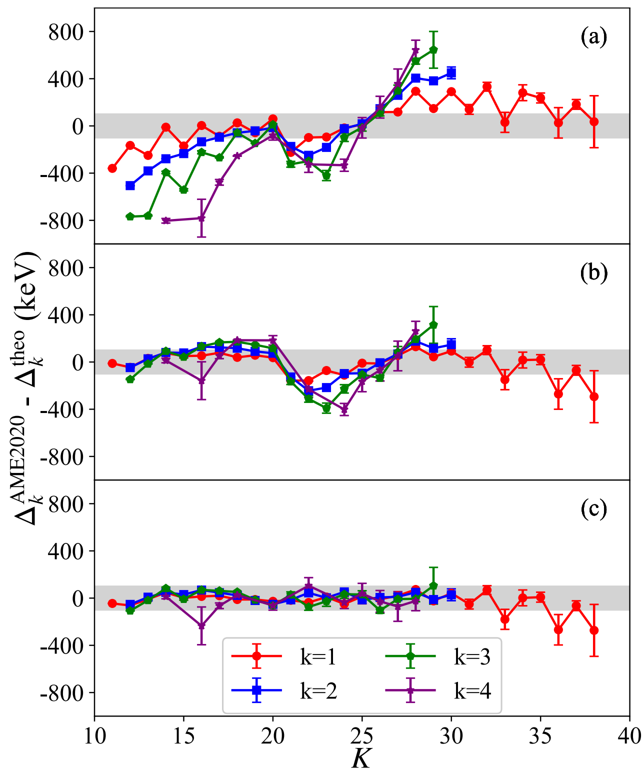

FIG. 1. Deviations of Δ_k between the experimental data in AME2020 [29] and the theoretical values obtained using (a) Eq. (4), (b) Eq. (7), and (c) Eq. (9) (in units of keV). The circles in red, squares in blue, pentagons in green, and nablas in purple represent the mirror nuclei with $k = 1, 2, 3, 4$, respectively. The gray strip indicates the region of deviations below 100 keV. The RMSDs of Eqs. (4), (7), and (9) are 310 keV, 147 keV, and 70 keV, respectively. If we exclude five data values with experimental uncertainties larger than 100 keV, the RMSD of Eq. (9) is reduced to only 49 keV.

The third and fourth terms in the above formula arise from the exchange and Coulomb pairing terms, respectively. This inclusion leads to a notable enhancement in the theoretical description of Δ_k, yielding an RMSD of ≈150 keV. Figures 1(a) and 1(b) show the deviations of Δ_k between the experimental data and the theoretical values obtained using Eqs. (4) and (7), respectively, for mirror nuclei with $A > 20$ and $k = 1, 2, 3, 4$. In Fig. 1(a), we see odd-even staggering for the cases of $k = 1$ and 3, while no staggering is observed for $k = 2$ and 4. This phenomenon is explained by the fourth term in Eq. (7), i.e., the Coulomb pairing effect. We noticed that in the mass relation formulas proposed in Refs. [24–27], the mass difference between a proton and a neutron was treated as an adjustable parameter without proper explanation. In this work, we elucidate the source of the Coulomb exchange term.

One of the purposes of this work is to obtain reliable predictions of the mass difference, we further introduce a shell correction term (denoted by δ_{sh} here) into Eq. (7), which is explained as follows. In Figs. 1(a) and 1(b), we observe a gradual increase in the deviation of Δ_k after $K = 8 + k$, followed by a sudden drop at $K = 21$, and a subsequent rise beyond $K = 20 + k$. This drop in Δ_k at $K = 21$ might be attributed to an *sd*-*pf* cross-shell effect, which occurs due to

TABLE I. Parameters of Eq. (9) obtained by a χ^2 fitting to the experimental data from AME2020 [29]. The parameters of the shell correction term, a_{sh1} and a_{sh2}, are presented with different magic numbers, respectively. All results are in the unit of keV, except for α which is dimensionless.

a_c	a_{ex}	a_p	α
670.1	−127.1	1029	1.1870
Shell		a_{sh1}	a_{sh2}
$(K_0, K1) = (8, 20)$		−304.1	17.91
$(K_0, K1) = (20, 28)$		−330.2	39.82
$K_0 = 20$		−183.3	–
$K_0 = 28$		−0.7	–

the relatively weaker Coulomb interaction between the $0d_{3/2}$ and $0f_{7/2}$ orbits [30], as well as the influence of the relativistic electromagnetic spin-orbit potential [31,32]. A similar sudden drop is also observed at $K = 9$, which can be attributed to a *p-sd* cross-shell effect. Based on this observation, we empirically obtain the shell correction term as follows:

$$\delta_{\mathrm{sh}} = \begin{cases} k^{\alpha}[a_{\mathrm{sh1}} + a_{\mathrm{sh2}}(K - K_0)], & \text{if } K_0 + k \leqslant K \leqslant K_1, \\ k^{\alpha}\, a_{\mathrm{sh1}}, & \text{if } K_0 < K < K_0 + k. \end{cases} \tag{8}$$

The above equation presents two distinct cases "in shell" and "cross shell", respectively. In the case of the in shell, K_0 and K_1 are adjacent magic numbers that define the boundaries of a major shell, and $K_0 + k \leqslant K \leqslant K_1$ indicates that both the neutron and proton numbers of the nuclei are in the same major shell between the magic numbers K_0 and K_1. In the case of the cross shell, K_0 is a magic number, and $K_0 < K < K_0 + k$ indicates that either the neutron or proton number is smaller that the magic number K_0 while the other is larger than K_0. α, a_{sh1}, a_{sh2} are free parameters. Our data fitting procedure yields an estimate of $\alpha \approx 1$, suggesting that the shell correction is approximately proportional to the difference between neutron and proton numbers.

Including δ_{sh} into Eq. (7), we finally have

$$\Delta_k(K) \approx a_c k(A-1)A^{-1/3} + f_k(K) + \frac{2^{5/3}}{3} a_{\mathrm{ex}} k + a_p(1-(-1)^k)(-1)^K A^{-1} + \delta_{\mathrm{sh}}. \tag{9}$$

In Table I, we present the six parameters, namely, a_c, a_{ex}, a_p, α, a_{sh1}, and a_{sh2}, of Eq. (9). These parameters are determined by a χ^2 fitting to the data from AME2020. In Fig. 1(c), we see a good agreement between the experimental data and the theoretical values obtained using Eq. (9); the RMSD is 70 keV. If we exclude five data values with experimental uncertainties exceeding 100 keV, corresponding to the mirror pairs ^{28}S - ^{28}Mg, ^{50}Co - ^{50}V, ^{55}Cu - ^{55}Fe, ^{71}Kr - ^{71}Br, and ^{75}Sr - ^{75}Rb, the RMSD decreases further to 49 keV. In Figs. 1(b) and 1(c), it is observed that the odd-even staggering effect of Δ_k for nuclei with $K \geqslant 30$ and $k = 1$ does not seem to be reasonably described by the Coulomb pairing term introduced in Eqs. (6), (7), and (9). This discrepancy can be resolved by incorporating the more recent experimental data. A detailed discussion of this issue will be presented in the subsequent section.

TABLE II. The RMSDs (in the unit of keV) of atomic masses extrapolations from the AME2012 [33] and AME2016 databases [34], respectively, to AME2020 [29]. "#" denotes the number of masses for comparison.

Database	Comparison to	RMSD	#
AME2012	AME2020	85	8
AME2016	AME2020	49	7

III. MASS PREDICTION AND DISCUSSION

In this section, we use Δ_k to make predictions for the atomic masses of neutron-deficient nuclei with $A > 20$ and $k = 1, 2, 3, 4$. We denote the Δ_k values obtained from Eq. (9) as Δ_k^{theo}, and have

$$M_{\mathrm{A}}^{\mathrm{pred}}(K-k, K) = M_{\mathrm{A}}(K, K-k) + \Delta_k^{\mathrm{theo}}(K). \tag{10}$$

Using Eq. (10), we can predict the mass of a nucleus with neutron number $K - k$ and proton number K by employing Δ_k^{theo} and the mass of the corresponding mirror nucleus.

One of the main purposes of this work is to demonstrate the predictive capability of our mass formula, i.e., Eq. (10). We exemplify this by carrying out mass extrapolations based on the AME2012 database [33] and comparing the result to the more recent AME2020 data. The detailed procedure is as follows. First, we determine the parameters a_c, a_{ex}, a_p, α, a_{sh1}, and a_{sh2} in Eq. (9) by a χ^2 fitting to the experimental data from AME2012. Next, we use these fitted parameters to calculate Δ_k^{theo}, and further predict the masses of neutron-deficient nuclei that were not available in the AME2012 database using Eq. (10) (the experimental mass values of the corresponding mirror nucleus are taken from AME2012). Out of these predicted masses, eight have been measured and compiled in AME2020. Figure 2 shows our predicted mass values, as well as the associated theoretical uncertainties, of the eight nuclei. The procedure for evaluating these theoretical uncertainties is presented in the Appendix. The mass values predicted by the Audi-Wapstra extrapolation in 2012 (denoted by AW2012) [33] and those predicted using the local correlation approach [28] are also presented for comparison. A good agreement of our result with the experimental data is observed. The RMSD derived from our mass extrapolations is 85 keV (see in Table II), which is significantly lower compared to the RMSD of 446 keV obtained from AW2012. While the work in Ref. [28] has achieved superior accuracy, our predictions has produced results that are competitively precise. We also see that the theoretical uncertainties of our extrapolations are small, due to the accuracy of Eq. (10) and the typically small experimental uncertainties associated with the masses of the corresponding neutron-rich mirror nuclei.

Similarly, we extend our investigation to cover the extrapolations from AME2016 to AME2020. Specially, we

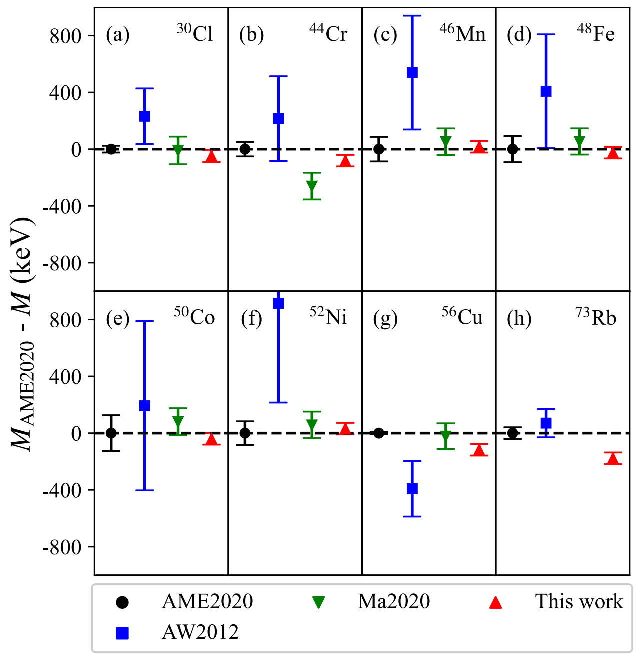

FIG. 2. Comparison of atomic masses (in the unit of keV) of neutron-deficient nuclei from the experimental data in AME2020 [29], the extrapolations from AW2012 [33], the extrapolations using the local correlation approach (i.e., Ma2020) [28], and the extrapolations using Eq. (10) in this work based on the AME2012 database. Our prediction exhibit a good agreement with the experimental data.

predict the masses of neutron-deficient nuclei that were not included in the AME2016 database [34] by utilizing parameters determined based on the AME2016 data. Out of these predicted masses, seven have been measured and compiled in AME2020. Impressively, the RMSD is only 49 keV (see in Table II).

Since the AME2020 database was published, new mass measurements were performed with high accuracy for the ground states of 12 nuclei, ^{58}Zn, ^{60}Ga, ^{61}Ga, ^{62}Ge, ^{63}Ge, ^{64}As, ^{65}As, ^{66}Se, ^{67}Se, ^{70}Kr, ^{71}Kr, and ^{75}Sr, at the HIRFL-RIBLL2-CSRe [35] and TITAN-MR-TOF [36] facilities, respectively. We also predict the masses of these nuclei using Eq. (10) by utilizing parameters optimized based on the AME2020 data. Figure 3 and Table III compare the data from the new measurements [35,36], AME2020, AW2020, and our result. The RMSD of our result with respect to the new data in Ref. [35] is 81 keV. For nuclei ^{64}As, ^{70}Kr, and ^{75}Sr, whose experimental uncertainties exceed 100 keV, our predicted values are −39562(41) keV, −41333(41) keV, and −46356(41) keV, respectively. If we exclude these three nuclei, the RMSD of our result with respect to the new data in Ref. [35] is reduced to 59 keV. For ^{65}As and ^{71}Kr, our predictions deviate from the new data in Ref. [35] by 46(59) keV and −12(49) keV, respectively. These deviations are much smaller compared to the deviations observed between the AME2020 data and the new data, which are −131(95) keV for ^{65}As and −271(132) keV for ^{71}Kr. Interestingly, for ^{60}Ga and ^{61}Ga, our predictions

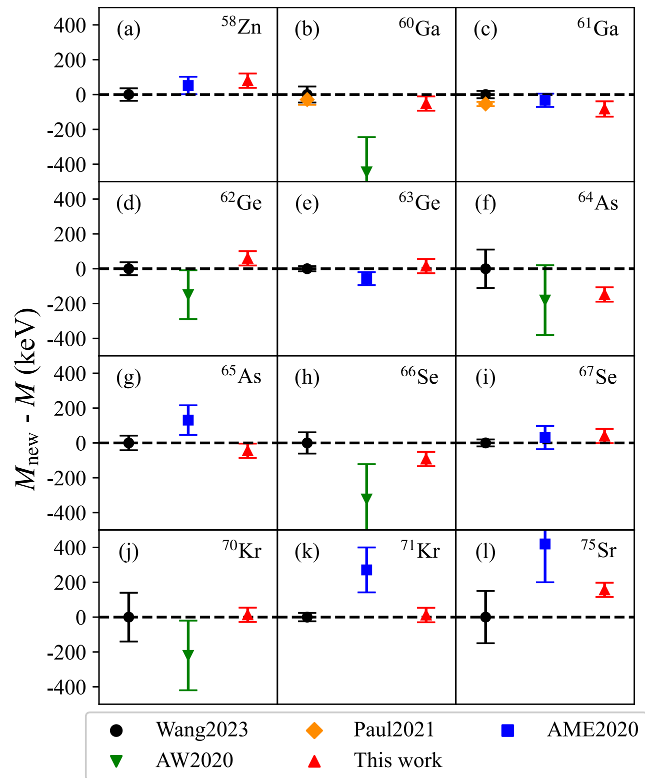

FIG. 3. Comparison of atomic masses (in the unit of keV) from the new experimental data in the references of Wang2023 [35] and Paul2021 [36], the experimental data in AME2020 [29], the results predicted in AW2020 [29], and the results predicted using Eq. (10) in this work based on the AME2020 database. Our results exhibit a remarkable agreement with the data in Wang2023 [35] and Paul2021 [36].

TABLE III. Atomic masses (in the unit of keV) of ^{58}Zn, ^{60}Ga, ^{61}Ga, ^{62}Ge, ^{63}Ge, ^{64}As, ^{65}As, ^{66}Se, ^{67}Se, ^{70}Kr, ^{71}Kr, and ^{75}Sr obtained from the very recent experimental data in Refs. [35,36], the experimental data in AME2020 [29], the results predicted in AW2020 [29], and the results predicted using Eq. (10) in this work based on the AME2020 database.

Nuclei	Ref. [35]	Ref. [36]	AME/AW2020	This work
^{58}Zn	−42248(36)	-	−42330(50)	−42327(41)
^{60}Ga	−40034(46)	−40005(30)	−39590(200)[a]	−39982(41)
^{61}Ga	−47168(21)	−47114(12)	−47135(38)	−47085(44)
^{62}Ge	−42289(37)	-	−42140(140)[a]	−42349(41)
^{63}Ge	−46978(15)	-	−46921(37)	−46993(41)
^{64}As	−39710(110)	-	−39530(200)[a]	−39562(41)
^{65}As	−46806(42)	-	−46937(85)	−46760(41)
^{66}Se	−41982(61)	-	−41660(200)[a]	−41890(41)
^{67}Se	−46549(20)	-	−46580(67)	−46588(41)
^{70}Kr	−41320(140)	-	−41100(200)[a]	−41333(41)
^{71}Kr	−46056(24)	-	−46327(129)	−46068(42)
^{75}Sr	−46200(150)	-	−46620(220)	−46356(41)

[a]Masses extrapolated from AW2020.

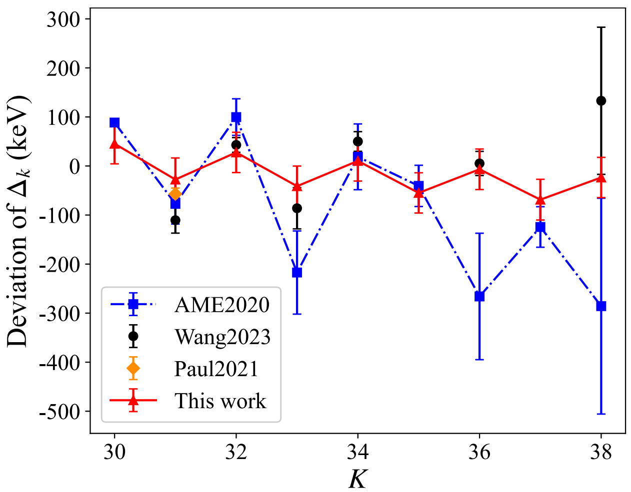

FIG. 4. Deviation of Δ_k derived using the experimental data in AME2020 [29], the new data in Wang2023 [35] and Paul2021 [36], and Eq. (9) from the function, $696A^{2/3} - 1505$ keV. Here, we emphasize the odd-even staggering phenomenon.

show slightly better agreement with the new data in Ref. [36] when compared to the data in Ref. [35].

Now, let us return to the issue of the odd-even staggering in Δ_k for nuclei with $K \geqslant 30$ and $k = 1$, which was discussed in the end of the previous section. To highlight the odd-even staggering, we subtracted an approximate function $696\,A^{2/3} - 1505$ keV from each Δ_k value. Figure 4 presents the deviations of Δ_k derived using the experimental data in AME2020, the new data in Refs. [35,36], and Eq. (9) from the function. Interestingly, we observe that the AME2020 data exhibit an odd-even staggering inverse specifically at $K = 35$. However, this inverse is not observed in the new data nor in our predictions. Our results agree well with the new data, further supporting the validity of the Coulomb pairing term introduced in this work.

Last but not least, encouraged by the remarkable agreement between our results and experimental data, we have included final mass predictions for a total of 174 neutron-deficient nuclei in the Supplemental Material of this paper [37]; 94 of these nuclei are currently unavailable for experimental measurement. The predictions are obtained by utilizing parameters optimized based on the data from AME2020 and Refs. [35,36] (with an RMSD of 55 keV). Our predictions cover a range of nuclei with $20 < A < 115$ and $k = 1, 2, 3, 4$. It is worth mentioning Ref. [27] here, which reports a relatively smaller Coulomb energy in neutron-deficient nuclei beyond the proton-drip line, particularly for those with $A < 20$. Taking this effect into account could potentially improve our results, which we leave to future work.

In Table IV we present a selected set of data that is of significant importance in astrophysics or has large experimental uncertainties. For comparison, we also include the predicted results from the Supplemental Material of Refs. [27] and [28]. Here, we provide a few examples. The reported mass values in AME2020 for ^{28}S, ^{50}Co, ^{55}Cu, ^{71}Kr, and ^{75}Sr are 4073(160) keV, −17589(126) keV, −31635(156) keV, −46327(129) keV, and −46619(220) keV, respectively. The new measurement [35] provides updated mass values for ^{71}Kr and ^{75}Sr, which are −46056(24) keV and −46200(150) keV, respectively. Our final predictions for these nuclei are 4308(41) keV, −17517(41) keV, −31740(41) keV, −46064(41) keV, and −46351(41) keV, respectively. For these nuclei, the predicted values from Refs. [27] and [28] align closely with our results, except for ^{50}Co. Although there are currently substantial discrepancies between the predictions and the experimental data for ^{28}S, ^{50}Co, ^{55}Cu, and ^{75}Sr, these gaps are expected to diminish as more accurate data becomes available in the future.

IV. SUMMARY

In this paper, we have studied the mass relation of mirror nuclei, Δ_k, and utilize these results to predict masses. To improve the accuracy of our predicted Δ_k, we take the Coulomb energy term in the Weizsäcker formula, and introduce several corrections. The key corrections mainly involve the Coulomb pairing and shell effects. We observe a prominent odd-even staggering phenomenon in Δ_k, and we successfully quantifies it through the Coulomb pairing term. Additionally, we find that cross-shell mirror nuclei tend to exhibit relatively lower mass differences. With the consideration of these corrections, we propose a formula for Δ_k that yields an RMSD of 70 keV compared to the experimental data from AME2020. Furthermore, if we exclude 5 data values with experimental

TABLE IV. Comparison of atomic masses (in keV) for ^{28}S, ^{50}Co, ^{55}Cu, ^{63}Ge, ^{65}As, ^{67}Se, ^{71}Kr, and ^{75}Sr. The mass values are taken from the experimental data in Ref. [35] and AME2020 [29], as well as the predicted results in the Supplemental Material of Refs. [27] and [28] and this work [37]. The predicted results in this work are derived using parameters optimized based on the data from AME2020 and Refs. [35,36].

Nuclei	Ref. [35]	AME2020 [29]	Ref. [27]	Ref. [28]	This work [37]
^{28}S	-	4073(160)	4359(68)	4205(86)	4308(41)
^{50}Co	-	−17589(126)	−17688(73)	−17685(86)	−17517(41)
^{55}Cu	-	−31635(156)	−31746(68)	−31798(82)	−31740(41)
^{63}Ge	−46978(15)	−46921(37)	−47010(96)	-	−46992(41)
^{65}As	−46806(42)	−46937(85)	−46751(96)	-	−46760(41)
^{67}Se	−46549(20)	−46580(67)	−46581(96)	-	−46586(41)
^{71}Kr	−46056(24)	−46327(129)	−46037(96)	-	−46064(41)
^{75}Sr	−46200(150)	−46620(220)	−46302(96)	-	−46351(41)

uncertainties larger than 100 keV, the RMSD reduced to only 49 keV.

We utilize our predicted values of Δ_k to predict atomic masses of neutron-deficient nuclei, using the mass formula Eq. (10). We have demonstrated strong predictive power of this formula through numerical experiments. We compare our mass extrapolations based on the AME2012 (AME2016) database with the more recent AME2020 data, and the RMSD is found to be 85 (49) keV. Moreover, when compared to the new experimental mass data reported in Ref. [35], our results yield an RMSD of 81 keV, which further reduces to 59 keV if excluding three data values with experimental uncertainties larger than 100 keV.

Finally, we have included our mass predictions for a total of 174 neutron-deficient nuclei, covering the range of nuclei with mass numbers between 20 and 115, in the Supplemental Material of this paper [37]. We believe the proposed mass formula raised in this paper and our predicted atomic masses will be very useful in the fields of astrophysics and nuclear structure for future studies. Further improvements can be achieved by refining the mass relation and incorporating more precise experimental data when it becomes available.

ACKNOWLEDGMENTS

The authors thank Prof. Y. M. Zhao, Prof. M. Bao, C. Ma for their valuable discussions, which greatly contributed to the improvement of this paper. The authors also acknowledge C. Ma for providing the predicted masses using the local correlation approach mentioned in Ref. [28]. This material is based upon work supported by the National Natural Science Foundation of China under Grants No. 12075169, No. 12322506, No. 12035011, and No. 11975167, and the National Key R&D Program of China under Grant No. 2018YFA0404403.

APPENDIX: χ^2 FITTING PROCEDURE WITH THE MAXIMUM-LIKELIHOOD METHOD

We denote experimental mass data by M_i^{expt} and experimental uncertainty by σ_i^{expt}, where i is an abbreviation of neutron and proton numbers; $i = 1, 2, \ldots, n$, and n is the number of data. We denote a mass formula by

$$M_i^{\text{theo}} = M(i; a_1, a_2, \ldots, a_t), \tag{A1}$$

where $a_1, a_2, \ldots, a_t$ are t parameters to be determined.

In this work, the χ^2 statistic is defined by

$$\chi^2 = \sum_{i=1}^{n} w_i \big(M_i^{\text{expt}} - M_i^{\text{theo}}\big)^2. \tag{A2}$$

Here, the weight, w_i, is given by

$$w_i = \frac{1}{(\sigma^{\text{theo}})^2 + \big(\sigma_i^{\text{expt}}\big)^2}, \tag{A3}$$

where σ^{theo} is the model error, which represents the deviation of the present formula from "the exact theory". In Ref. [9] σ^{theo} is evaluated by decoupling the experimental uncertainty from variance using the maximum-likelihood method:

$$(\sigma^{\text{theo}})^2 = \frac{\sum_{i=1}^{n} w_i^2 \big[\big(M_i^{\text{expt}} - M_i^{\text{theo}}\big)^2 - \big(\sigma_i^{\text{expt}}\big)^2\big]}{\sum_{i=1}^{n} w_i^2}. \tag{A4}$$

The parameters $a_1, a_2, \ldots, a_t$ are determined by minimizing the χ^2 statistic in Eq. (A2), i.e., we solve the following equations:

$$\frac{\partial}{\partial a_j} \sum_{i=1}^{n} w_i \big(M_i^{\text{expt}} - M_i^{\text{theo}}\big)^2 = 0, \quad j = 1, 2, \ldots, t. \tag{A5}$$

Equations (A3)–(A5) are iteratively solved until the convergence is achieved for $a_1, a_2, \ldots, a_t$, w_i and σ^{theo}.

[1] D. Lunney, J. M. Pearson, and C. Thibault, Rev. Mod. Phys. **75**, 1021 (2003).

[2] K. Blaum, Phys. Rep. **425**, 1 (2006).

[3] J. Duflo and A. P. Zuker, Phys. Rev. C **52**, R23(R) (1995).

[4] C. Qi, J. Phys. G: Nucl. Part. Phys. **42**, 045104 (2015).

[5] S. Goriely, N. Chamel, and J. M. Pearson, Phys. Rev. Lett. **102**, 152503 (2009).

[6] S. Goriely, N. Chamel, and J. M. Pearson, Phys. Rev. C **93**, 034337 (2016).

[7] M. Liu, N. Wang, Y. Deng, and X. Wu, Phys. Rev. C **84**, 014333 (2011).

[8] N. Wang, M. Liu, X. Wu, and J. Meng, Phys. Lett. B **734**, 215 (2014).

[9] P. Möller, A. J. Sierk, T. Ichikawa, and H. Sagawa, At. Data Nucl. Data Tables **109**, 1 (2016).

[10] G. T. Garvey and I. Kelson, Phys. Rev. Lett. **16**, 197 (1966).

[11] G. T. Garvey, W. J. Gerace, R. L. Jaffe, I. Talmi, and I. Kelson, Rev. Mod. Phys. **41**, S1 (1969).

[12] J. Barea, A. Frank, J. G. Hirsch, and P. Van Isacker, Phys. Rev. Lett. **94**, 102501 (2005).

[13] J. Barea, A. Frank, J. G. Hirsch, P. Van Isacker, S. Pittel, and V. Velázquez, Phys. Rev. C **77**, 041304(R) (2008).

[14] G. Audi, A. H. Wapstra, and C. Thibault, Nucl. Phys. A **729**, 337 (2003).

[15] G. J. Fu, H. Jiang, Y. M. Zhao, S. Pittel, and A. Arima, Phys. Rev. C **82**, 034304 (2010).

[16] H. Jiang, G. J. Fu, Y. M. Zhao, and A. Arima, Phys. Rev. C **82**, 054317 (2010).

[17] G. J. Fu, Y. Lei, H. Jiang, Y. M. Zhao, B. Sun, and A. Arima, Phys. Rev. C **84**, 034311 (2011).

[18] H. Jiang, G. J. Fu, B. Sun, M. Liu, N. Wang, M. Wang, Y. G. Ma, C. J. Lin, Y. M. Zhao, Y. H. Zhang, Z. Ren, and A. Arima, Phys. Rev. C **85**, 054303 (2012).

[19] M. Bao, H. Jiang, and Y. M. Zhao, Nucl. Phys. Rev. **40**, 141 (2023).

[20] W. E. Ormand, Phys. Rev. C **55**, 2407 (1997).

[21] E. P. Wigner, in *Proceedings of the R. A. Welch Foundation Conference on Chemical Research*, edited by W. O. Millikan (R. A. Welch Foundation, Houston, 1957), Vol. 1.

[22] B. A. Brown, W. A. Richter, and R. Lindsay, Phys. Lett. B **483**, 49 (2000).

[23] B. A. Brown, R. R. C. Clement, H. Schatz, A. Volya, and W. A. Richter, Phys. Rev. C **65**, 045802 (2002).
[24] M. Bao, Y. Lu, Y. M. Zhao, and A. Arima, Phys. Rev. C **94**, 044323 (2016).
[25] Y. Y. Zong, M. Q. Lin, M. Bao, Y. M. Zhao, and A. Arima, Phys. Rev. C **100**, 054315 (2019).
[26] Y. Y. Zong, C. Ma, Y. M. Zhao, and A. Arima, Phys. Rev. C **102**, 024302 (2020).
[27] Y. Y. Zong, C. Ma, M. Q. Lin, and Y. M. Zhao, Phys. Rev. C **105**, 034321 (2022).
[28] C. Ma, Y. Y. Zong, Y. M. Zhao, and A. Arima, Phys. Rev. C **102**, 024330 (2020).
[29] M. Wang, W. Huang, F. Kondev, G. Audi, and S. Naimi, Chin. Phys. C **45**, 030003 (2021).
[30] B. A. Brown, Phys. Rev. C **43**, R1513(R) (1991).
[31] J. A. Nolen and J. P. Schiffer, Annu. Rev. Nucl. Sci. **19**, 471 (1969).
[32] M. Bentley and S. Lenzi, Prog. Part. Nucl. Phys. **59**, 497 (2007).
[33] M. Wang, G. Audi, A. H. Wapstra, F. G. Kondev, M. MacCormick, X. Xu, and B. Pfeiffer, Chin. Phys. C **36**, 1603 (2012).
[34] W. Huang, G. Audi, M. Wang, F. G. Kondev, S. Naimi, and X. Xu, Chin. Phys. C **41**, 030002 (2017).
[35] M. Wang, Y. H. Zhang, X. Zhou, X. H. Zhou, H. S. Xu, M. L. Liu, J. G. Li, Y. F. Niu, W. J. Huang, Q. Yuan, S. Zhang, F. R. Xu, Y. A. Litvinov, K. Blaum, Z. Meisel, R. F. Casten, R. B. Cakirli, R. J. Chen, H. Y. Deng, C. Y. Fu *et al.*, Phys. Rev. Lett. **130**, 192501 (2023).
[36] S. F. Paul, J. Bergmann, J. D. Cardona, K. A. Dietrich, E. Dunling, Z. Hockenbery, C. Hornung, C. Izzo, A. Jacobs, A. Javaji, B. Kootte, Y. Lan, E. Leistenschneider, E. M. Lykiardopoulou, I. Mukul, T. Murböck, W. S. Porter, R. Silwal, M. B. Smith, J. Ringuette *et al.*, Phys. Rev. C **104**, 065803 (2021).
[37] See Supplemental Material at http://link.aps.org/supplemental/10.1103/PhysRevC.109.014304 for the final mass predictions for neutron-deficient nuclei in this work.